MHD Modeling of CHI on NSTX

Xianzhu Tang
Los Alamos National Laboratory

Allen H Boozer
Columbia University

and
NSTX Research Team

Nov. 18, 2002

Overview

- Grad-Shafranov equilibrium modeling.
  - Grad-Shafranov model has flows!
  - Helicity and energy balance.

- Resistive steady state.
  - Unlike high-S Ohmic discharges, resistive steady state gives significantly different answer from Grad-Shafranov equilibrium modeling.
  - Reason: plasma flow scales with externally imposed voltage, not parallel resistivity.
  - Consequence: plasma inertia and viscous forces induce $\mathbf{j}_\perp$. Small $\mathbf{j}_\perp$ brings strong poloidal localization of large parallel current on a flux surface.

- Transient CHI for secondary current drive.
  - 2D forced reconnection.
  - Ramp down of 3D nonlinearly saturated state.

Open field line Grad-Shafranov Equi.

- Magnetic coordinates for open field lines,

$$\mathbf{B} = \nabla\psi\times\nabla\theta+\nabla\varphi\times\nabla\chi(\psi,t) = G(\chi)\nabla\varphi+\nabla\varphi\times\nabla\chi.$$

At electrode surfaces, $\mathbf{B}\cdot\mathbf{n} > 0, \theta = 0; \mathbf{B}\cdot\mathbf{n} < 0, \theta = 2\pi.$

- Grad-Shafranov equation is closed by specifying the parallel current from resistive Ohm's law,

$$\frac{dG}{d\psi} = \frac{\mathcal{V}(\psi)}{q(\psi)\mathcal{R}(\psi)}; \;\; \mathcal{R}(\psi) \equiv \int_0^{2\pi} \frac{\eta B^2}{\mathbf{B}\cdot\nabla\varphi} d\theta$$

- Helicity and energy balance ($\nabla p = 0$)

$$\begin{aligned} \mathcal{V}(\psi) &= -4\pi^2 q(\psi)\eta_{||}(G+\iota I)k_n; \\ \mathcal{V}(\psi)\frac{dG}{d\psi} &= 4\pi^2\eta_{||}(G+\iota I)k_n^2. \end{aligned}$$

Net parallel current $k_n = -dG/d\chi$.
G and I are poloidal and toroidal plasma current.

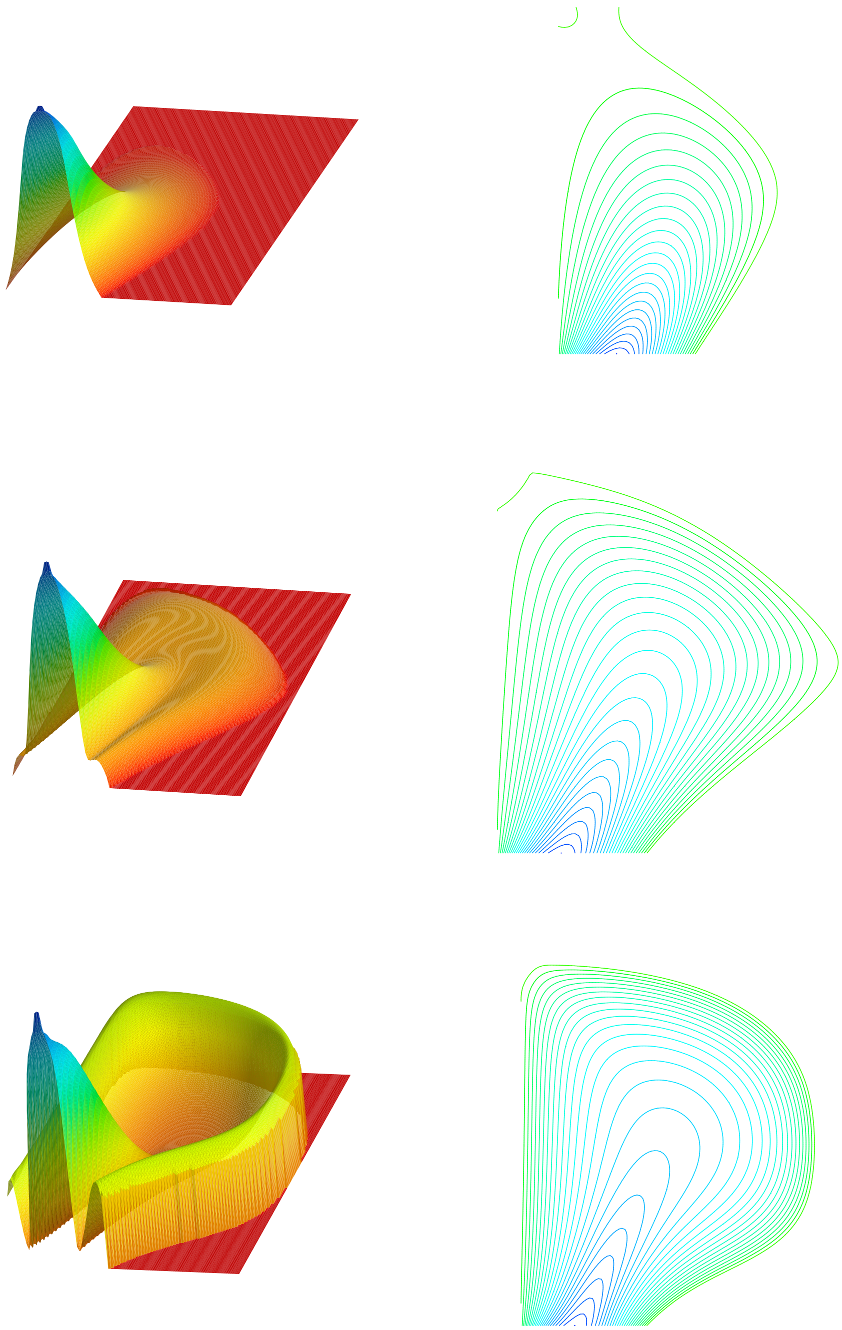

Figure 1: Surface plot of RJ_φ and contour plot of ψ (top $\mathcal{V} = -1$; middle $\mathcal{V} = -2$; bottom $\mathcal{V} = -4$.)

Interpretation and reconstruction

- Quasi-neutral modification of Φ is included in G-S model,
$$\Phi(\chi,\theta) = \mathcal{V}(\chi)\frac{\int_0^\theta \frac{\eta B^2}{\mathbf{B}\cdot\nabla\varphi}d\theta}{\int_0^{2\pi} \frac{\eta B^2}{\mathbf{B}\cdot\nabla\varphi}d\theta}.$$
In MHD, that implies a self-consistent $\mathbf{B}\times\nabla\Phi$ flow.

- In Ohmic discharges,
high $T_e \rightarrow$ large $S \rightarrow$ small $\mathcal{M}_g$.

- In CHI discharges,
$\mathbf{v} = \mathbf{B}\times\nabla\Phi/B^2$ independent of S, vanishing $\rho \rightarrow$ small $\mathcal{M}_g$.

- Due to the operational density limit in CHI, G-S model is a fragile limit for CHI.

- Reconstruction from experiments: EFIT, MFIT, ESC, TSC.

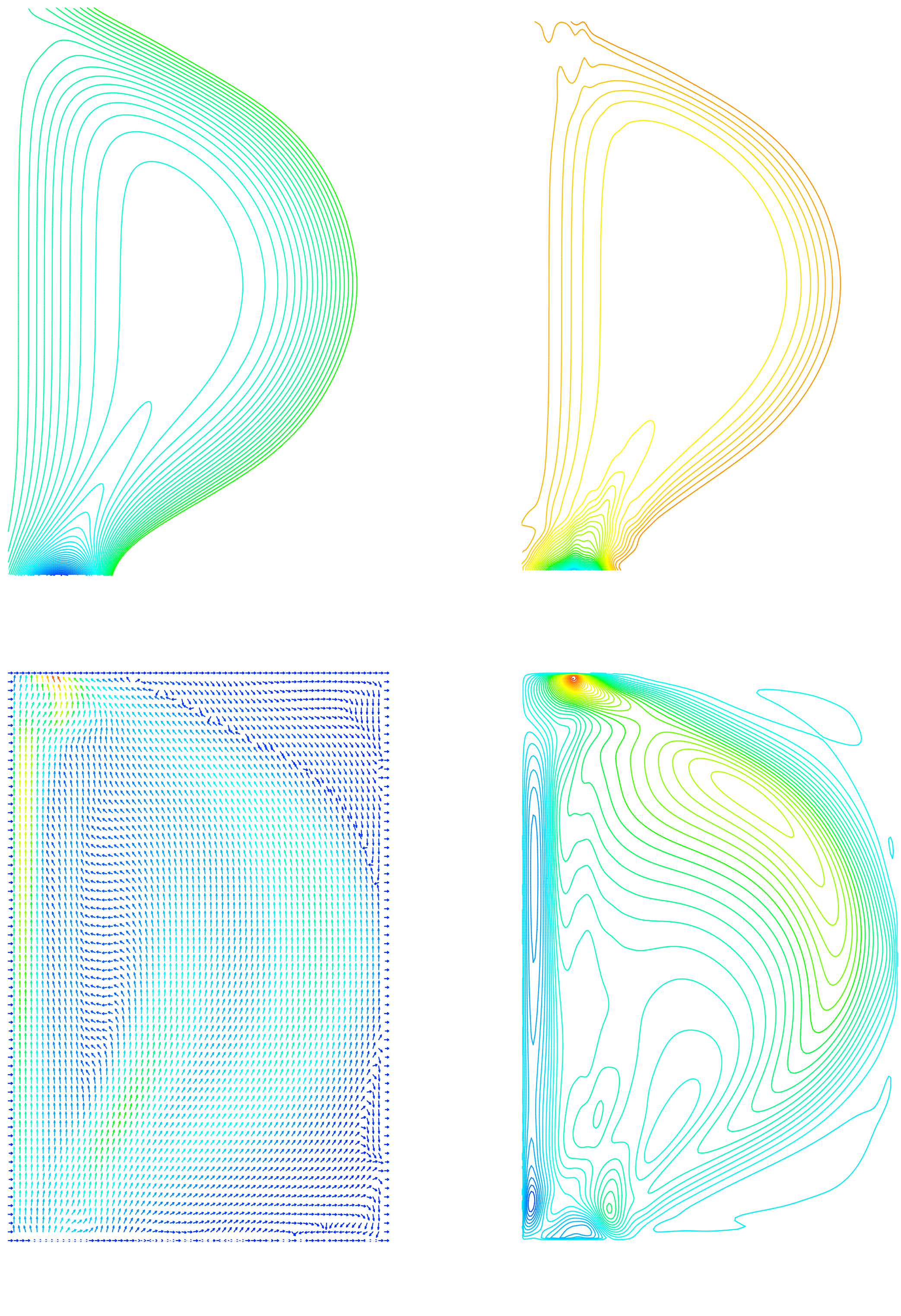

Figure 2: Top left: poloidal flux ψ; top right: RB_φ; Bottom left: poloidal flow; Bottom right: v_φ.

Resistive Steady State: $\mathbf{j}_\perp$

- $\mathbf{j}_\perp$ is required for force balance with plasma inertia and viscous force,

$$\mathbf{j} \times \mathbf{B} = \mathbf{F}; \;\; \mathbf{F} = \rho \mathbf{v} \cdot \nabla \mathbf{v} - \rho \nu \nabla^2 \mathbf{v}.$$

- Largest $\mathbf{j}_\perp$ occurs around the absorber and injector with electrode gap d,

$$j_\perp \sim \mathcal{M}_g^2 B/d, \;\; \mathcal{M}_g \equiv \frac{v_{\mathbf{E}\times\mathbf{B}}}{v_A} = g\frac{\rho^{1/2}\mathcal{V}}{dB^2}.$$

  Magnetic Mach number $\mathcal{M}_g$ depends on a geometric factor $g \sim 1 - \mathbf{E}\cdot\mathbf{B}/EB$.

- At the injector, poloidal field is designed to be maximumly aligned with $\mathbf{E}$ for high efficiency in driving the parallel current ($g \to 0$). Opposite is true at the absorber ($g \to 1$).

Resistive Steady State: $j_{\|}$

- Parallel current is the one affected most by flows,

$$k_{\|} \equiv \mathbf{j} \cdot \mathbf{B}/jB = k_n(\psi) + k_{ps}(\psi, \theta) + k_{\alpha\psi}(\psi, \theta).$$

- Net parallel current $k_n(\psi)$ is not affected by $\mathbf{j}_{\perp}$ or

$$\mathbf{F} = F_{\psi}(\psi, \theta)\nabla\psi + F_{\alpha}(\psi, \theta)\nabla\alpha.$$

Clebsch coordinates $\alpha \equiv \theta - \iota\varphi, \xi \equiv \theta + \iota\varphi$.

- Pfirsch-Schlüter current is driven by F_{ψ},

$$k_{ps} = \frac{2g_{\alpha\xi}}{qJ_m B^2}F_{\psi} - \frac{qJ_m}{2}F_{\psi}.$$

- $k_{\alpha\psi}$ current is driven by F_{α},

$$k_{\alpha\psi} = -\frac{2g_{\psi\xi}}{qJ_m B^2}F_{\alpha} + \int_0^{\theta} \frac{\partial}{\partial\psi}(qJ_m F_{\alpha})d\theta'.$$

Small $k_\perp \rightarrow$ large $k_\parallel$

- Normalized perpendicular current and magnetic field

$$k_\perp^\alpha \equiv \frac{\mathbf{j}_\perp \cdot \nabla\alpha}{\sqrt{g^{\alpha\alpha}}B} = \frac{F_\psi}{\sqrt{g^{\alpha\alpha}}B} \quad ; \quad k_\perp^\psi \equiv \frac{\mathbf{j}_\perp \cdot \nabla\psi}{\sqrt{g^{\psi\psi}}B} = -\frac{F_\alpha}{\sqrt{g^{\psi\psi}}B}.$$

$$b_\alpha = \mathbf{B} \cdot \frac{\partial \mathbf{x}}{\partial \alpha}/B\sqrt{g_{\alpha\alpha}} \quad ; \quad b_\psi = \mathbf{B} \cdot \frac{\partial \mathbf{x}}{\partial \psi}/B\sqrt{g_{\psi\psi}}.$$

- Pfirsch-Schlüter current $\sim q^2 k_\perp^\alpha$

$$k_{ps} = b_\alpha \sqrt{g_{\alpha\alpha} g^{\alpha\alpha}} k_\perp^\alpha - \frac{1}{2} q J_m \sqrt{g^{\alpha\alpha}} B k_\perp^\alpha$$

- $k_{\alpha\psi}$ current $\sim \frac{\partial}{\partial\psi}(qJ_m B\sqrt{g^{\psi\psi}})k_\perp^\psi$.

$$k_{\alpha\psi} = b_\psi \sqrt{g_{\psi\psi} g^{\psi\psi}} k_\perp^\psi - \int_0^\theta \frac{\partial}{\partial\psi}(qJ_m\sqrt{g^{\psi\psi}}Bk_\perp^\psi)d\theta'$$

- Strong parallel current is localized poloidally around injector where local B_θ is small on a high q field line, and around absorber where local B_θ is strong on a high q field line near the X point.

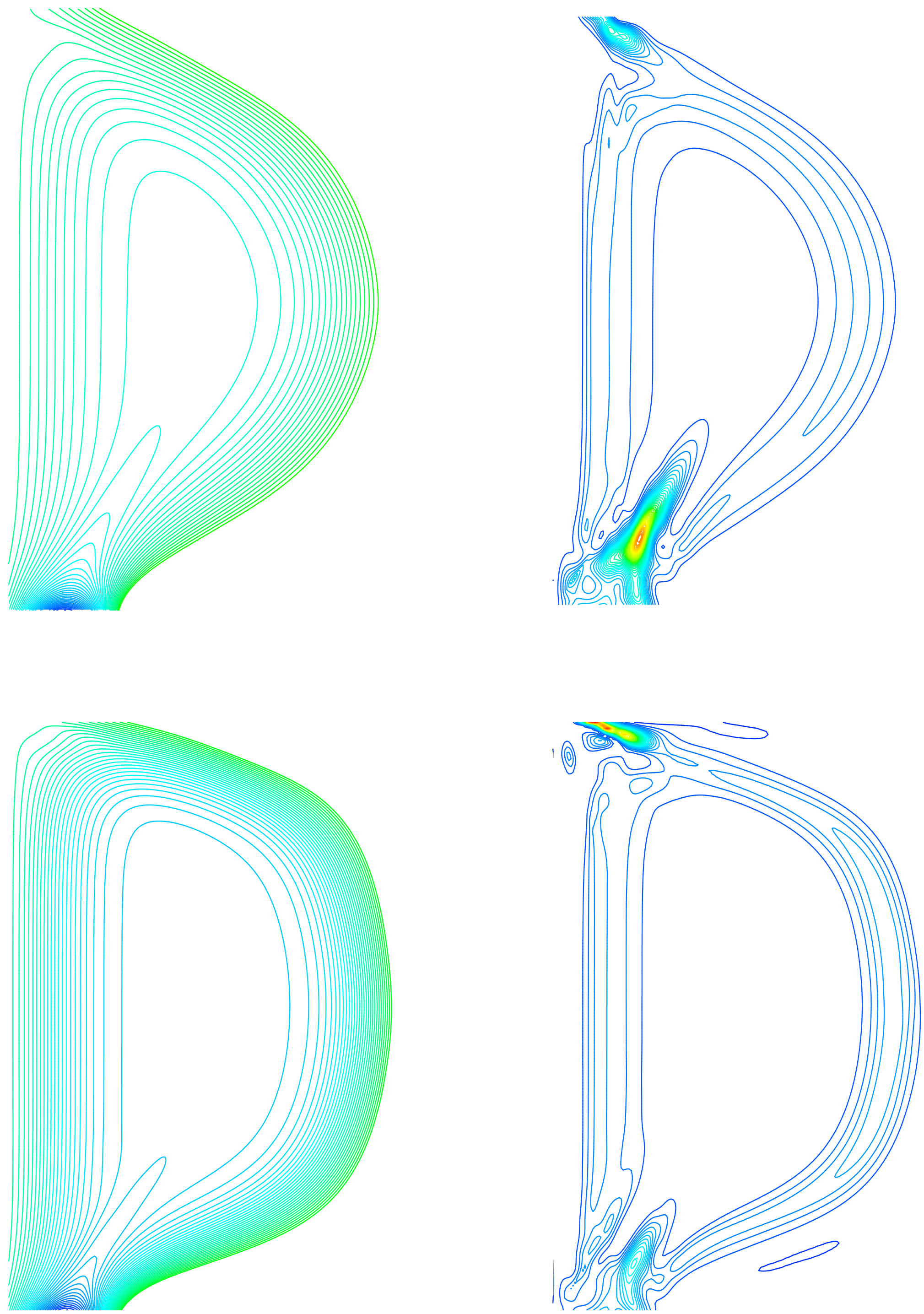

Figure 3: Left: poloidal flux ψ; right: $k_{\|}$. Bottom run has twice the voltage as the top run. In both cases, $k_{\|} \gg k_{\perp}$.

Transient CHI for secondary current drive

- Non-inductive startup is attractive for NSTX and future ST devices.
- CHI prepares the initial plasma and field. Secondary current drive provides profile control and sustainment.
- Secondary current drive (Ohmic, beam, rf wave) all require a plasma core with adequate confinement (closed flux surfaces).
- Steady state CHI plasma with good core confinement remains an issue of debate, but transient CHI plasma can easily satisfy the requirement.

2D or 3D?

- Transient axisymmetric CHI plasma: forced 2D reconnection to form large volume of axisymmetric plasmoid.
  - pinching off the injector flux or modulating the voltage.
  - downside: q profile is opposite of eventual ST profile, more work for secondary drive.

- Transient 3D CHI plasma: ramp-down a nonlinearly saturated high-$\mathcal{V}$ 3D plasma.
  - saturated $n = 0$ component has substantial current penetration into the core.
  - fast decay of $n > 0$ modes leaves $n = 0$ with ST-like q profile.
  - room for q profile optimization during the CHI phase.

Comparison numerical experiments

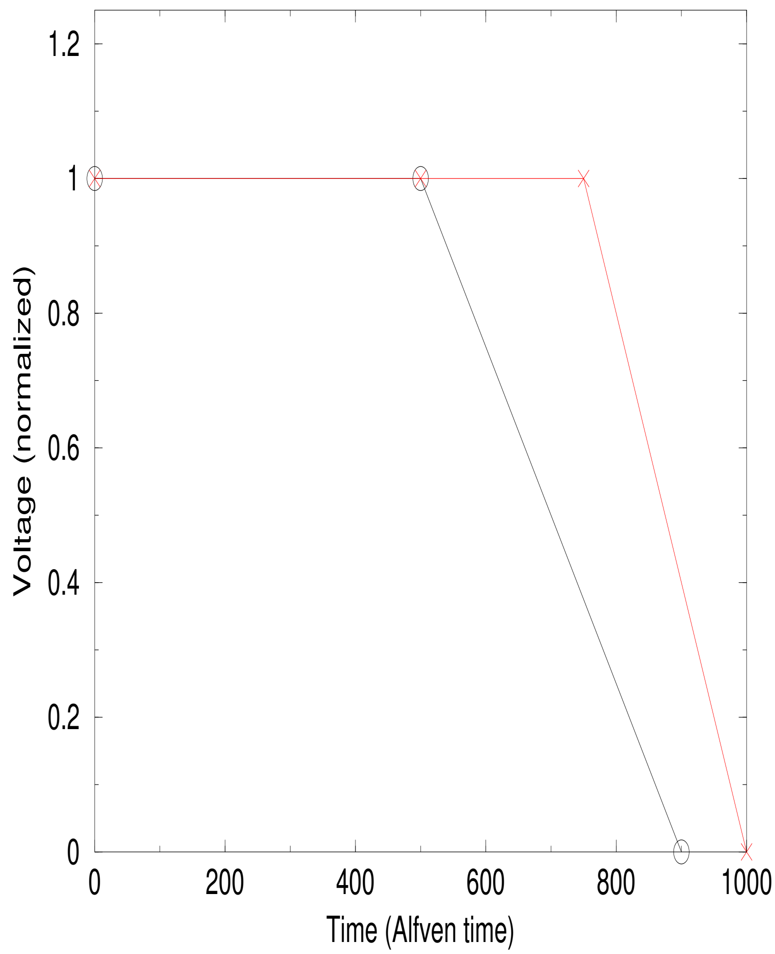

Figure 4: Two sequence of MHD calculations

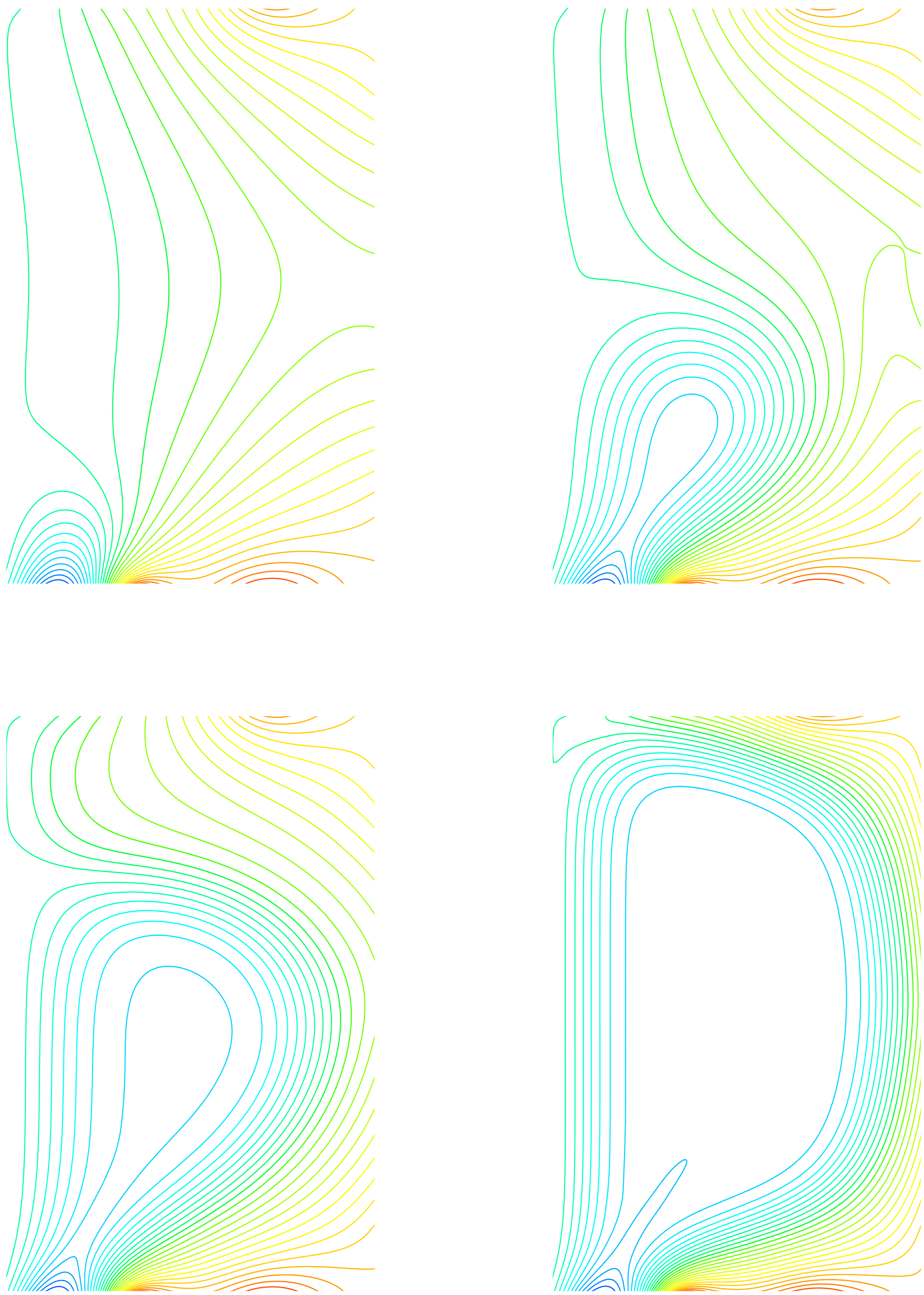

Figure 5: Axisymmetric ramp up to resistive steady state: poloidal Flux χ over time.

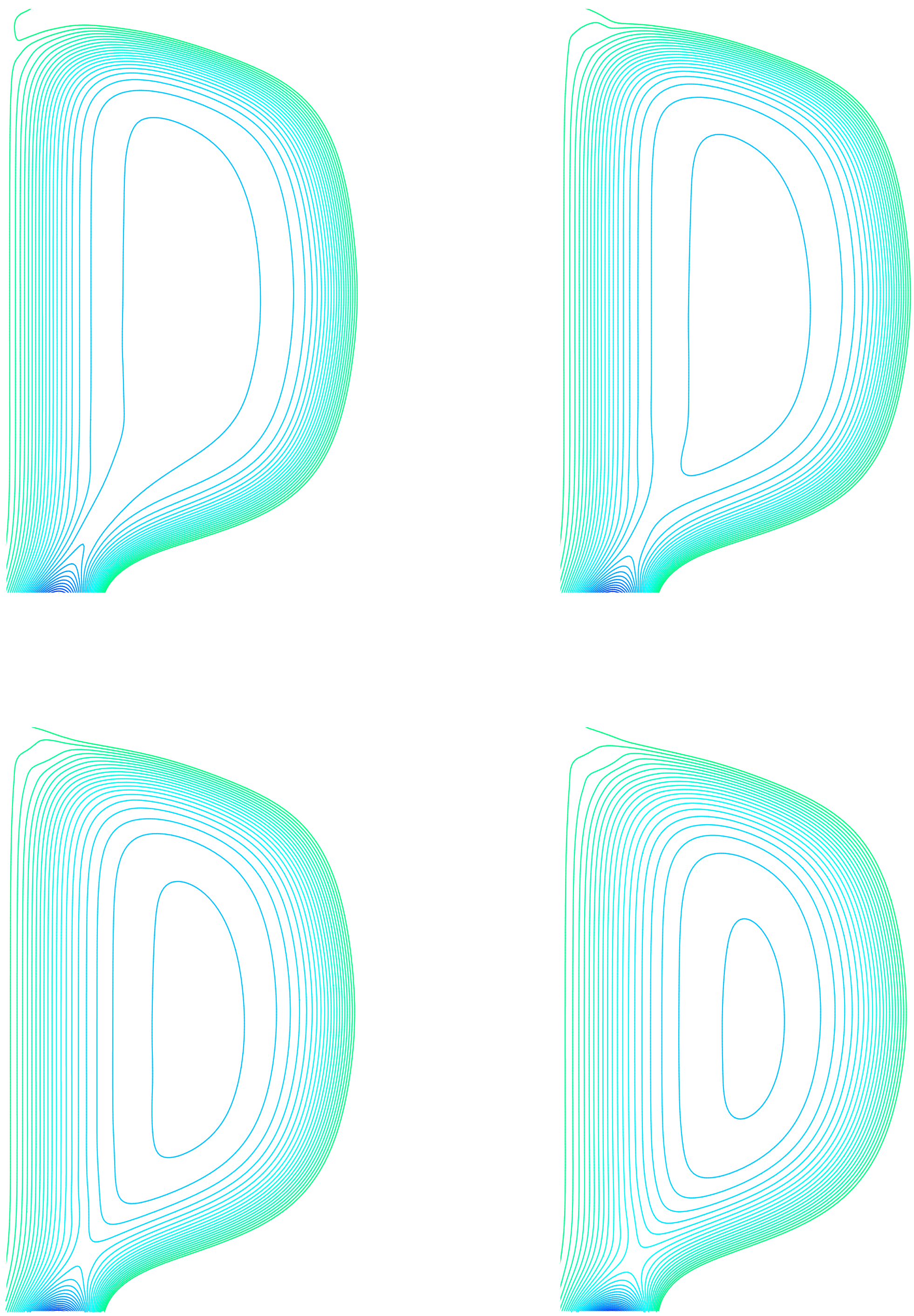

Figure 6: Axisymmetric ramp down: poloidal Flux χ over time. (forced 2D reconnection by voltage modulation)

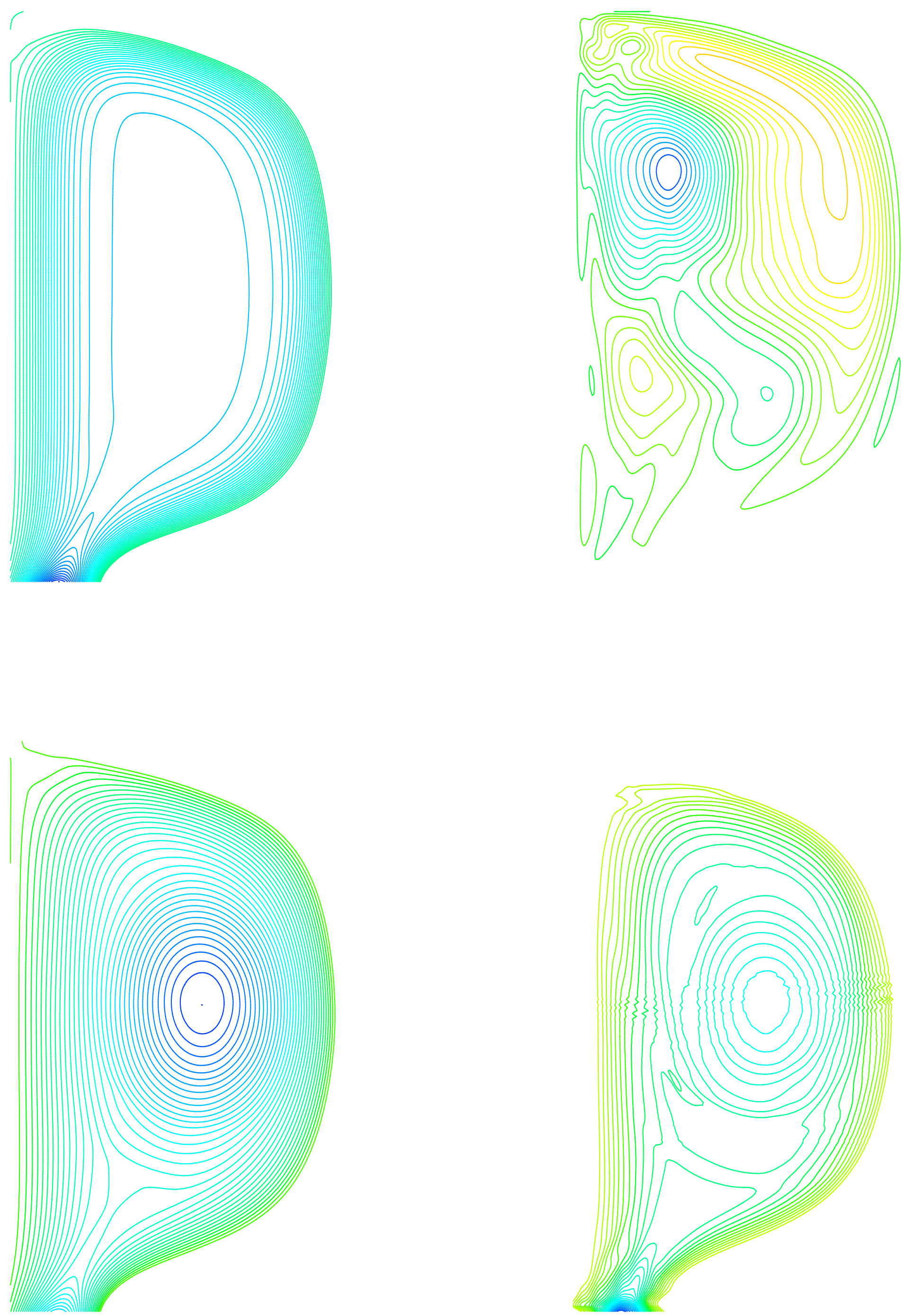

Figure 7: Kink instability and its nonlinear saturation

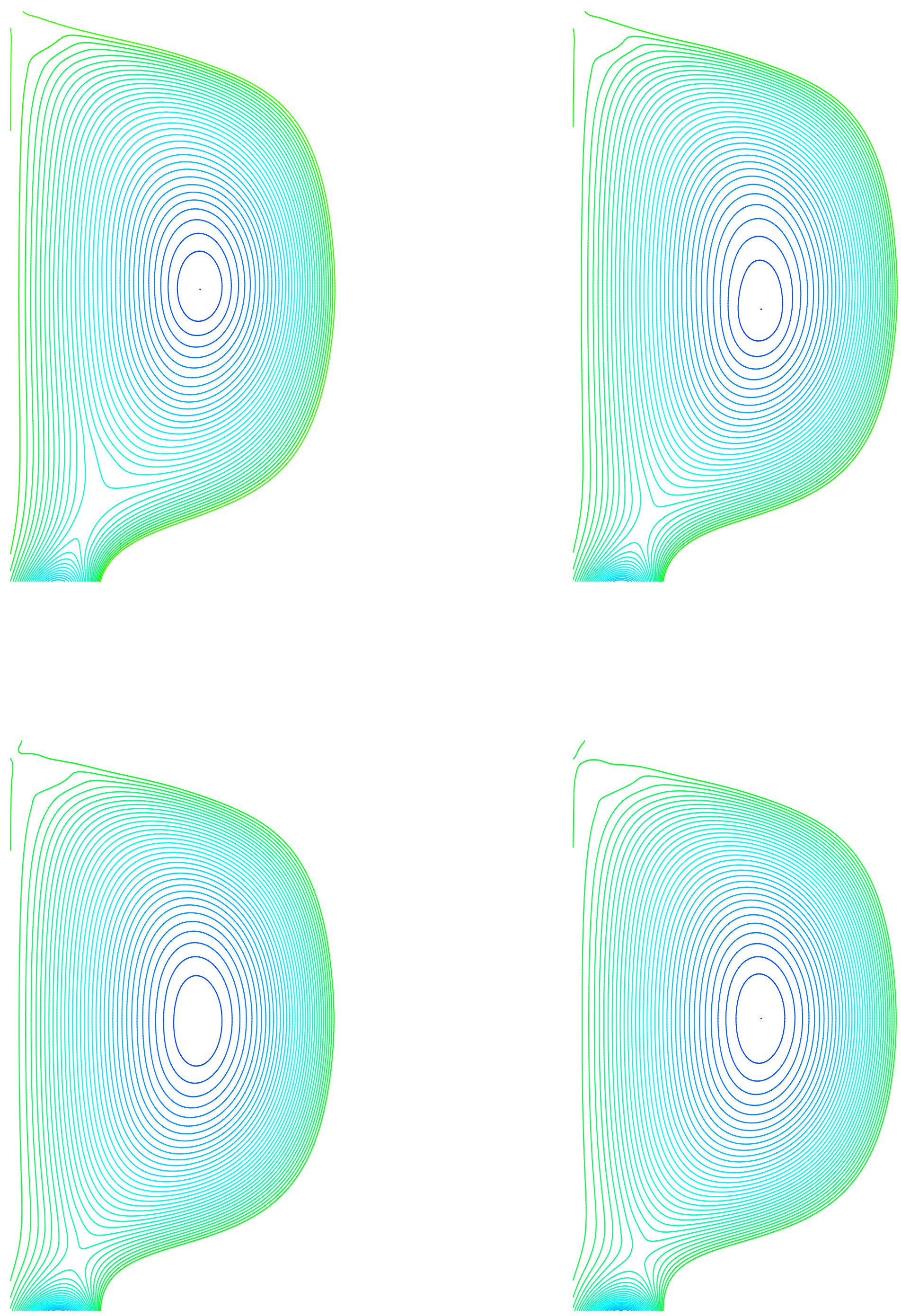

Figure 8: Ramp down of the nonlinearly saturated state

Freely decaying CHI plasma

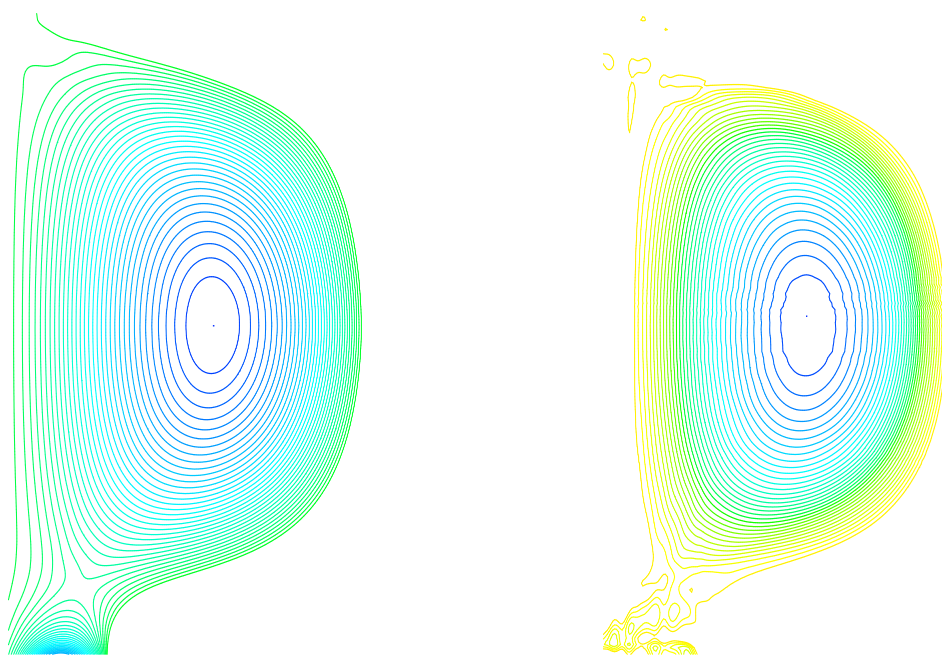

Figure 9: Freely decay CHI plasma (vanishing voltage), n=0 χ (left) and RB_φ (right).

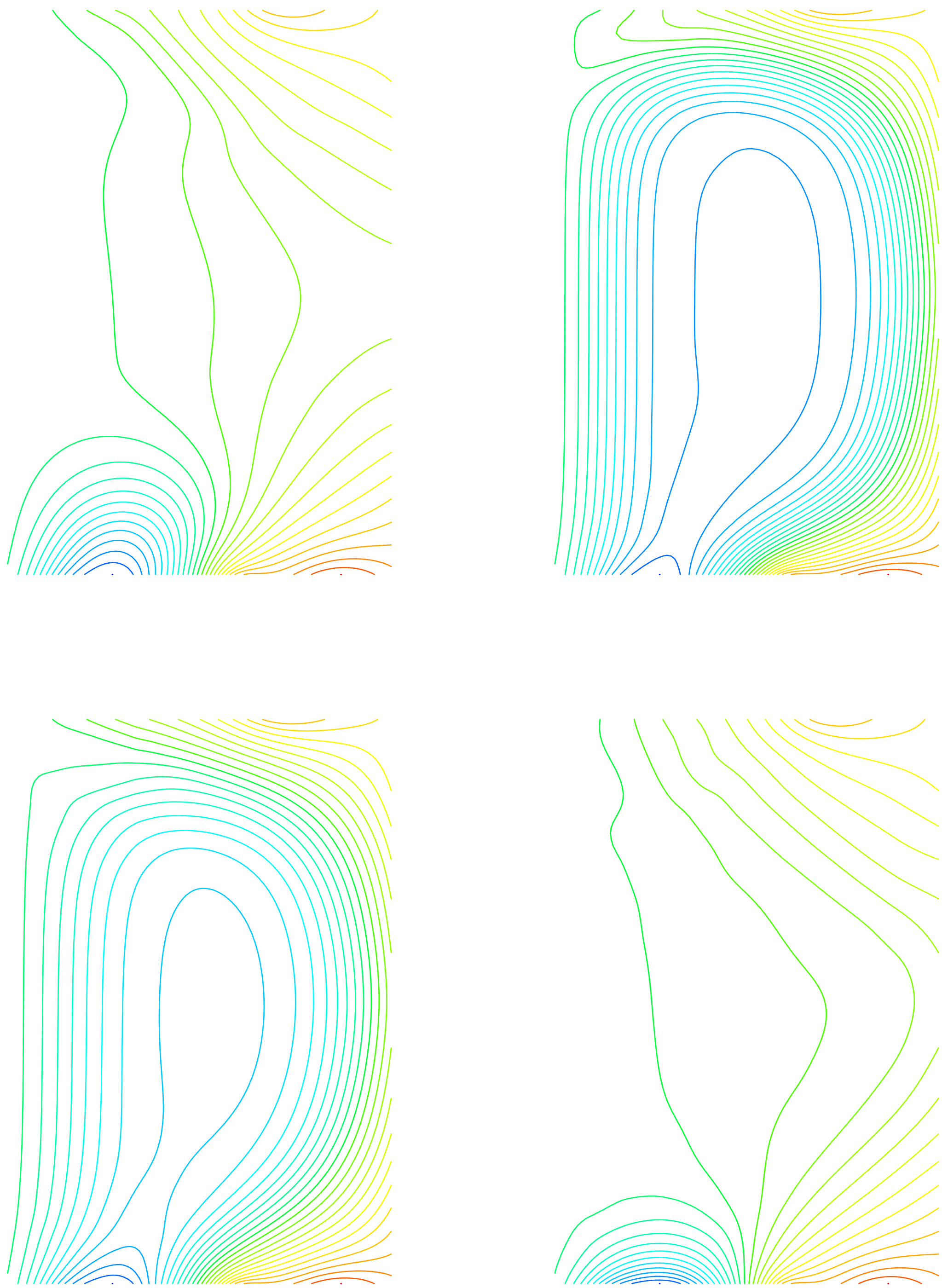

Figure 10: Ramp down could cause discharge termination. Freedom in PF shaping flux design. Top:Ramp-up; Down:Ramp-down